International Journal of Advanced Engineering and Management Research

Vol. 9, No. 03; 2024

ISSN: 2456-3676

Dynamic Deformation of the Fairing Under the Action of an External Distributed Load

Nina Antonenko[1], Dmytro Danylchenko[2], Andrii Zasovenko[3]

[1]National University Zaporizhzhia Polytechnic, Department of Mathematics,
64 Zhukovskoho St., Zaporizhzhia, 69063, Ukraine

[2]“DATAXDEV” LLC, Zaporizhzhia, Ukraine

[3]National University Zaporizhzhia Polytechnic, Department of Mathematics,
64 Zhukovskoho St., Zaporizhzhia, 69063, Ukraine

doi.org/10.51505/ijaemr.2024.9307 URL: http://dx.doi.org/10.51505/ijaemr.2024.9307

Received: May 14, 2024 Accepted: May 20, 2024 Online Published: Jun 01, 2024

Abstract
The problem of dynamic deformation of the fairing under the action of an external distributed load is considered. The fairing is represented as a hemisphere connected to a cylinder. The mathematical model of the processes of forced vibrations of the structure is reduced to the consideration of a hyperbolic system of nonlinear differential equations of the theory of shells and curvilinear rods of the Timoshenko type. The problem is numerically solved by the grid-characteristic method. Numerical results are obtained.

Keywords: shell, stress, deflection, Timoshenko's theory of shells, hyperbolic differential equation, grid-characteristic method.

1. Introduction

Composite piecewise-homogeneous shell structures are widely used in various fields of the national economy and modern technology. The development of scientific and technological progress, the introduction of new technologies, and the use of explosive energy set new tasks for researchers to study the behavior of such structures under intense dynamic loads. Elements of energy pipelines and components of solid rocket boosters are also designed for the action of non-stationary shock loads.

Currently, the numerical modeling of real physical processes is increasingly used. This is primarily due to the fact that numerical modeling is many times more cost-effective than conducting real experiments. Additionally, in some cases, it is difficult to construct a physical model that accurately represents a real engineering object with certain operational and technical characteristics. The aim of the researches is to increase the mechanical strength of the constructions by enabling the manufacture of structures with predetermined properties through variations in geometric dimensions and mechanical properties of their components.

Algorithms and programs for calculating composite shell structures under the action of stationary and dynamic loads are presented in the handbook (Myachenkov & Grigoriev, 1981). The monograph (Naval et al., 1986) is devoted to the dynamic behavior of composite shells under non-stationary loads. The dynamic behavior of the reinforced shells of revolution, taking into account the discrete arrangement of ribs, is studied in the article (Lugovoi & Meish, 1992). In the paper (Shulga & Bogdanov, 2003) the axisymmetric nonlinear vibrations of conical shells are studied. Forced vibrations of a truncated elliptic conical shell under distributed impulsive load, deriving linear equations from Timoshenko's theory and developing a numerical algorithm to explore its dynamic behavior is examined in the study (Meish et al., 2020). Problems of dynamic behavior of reinforced ellipsoidal shells are addressed in the paper (Meish, 2005). In study (Meish & Kairov, 2005), the dynamic problems for discretely reinforced shells with initial deflections are numerically solved. The dynamic problem for a sandwich cylindrical shell under distributed nonstationary loading is solved with regard for the discreteness of the core in (Lugovoy et al., 2005). Nonlinear dynamic stability investigations for isotropic and composite cylindrical shells under pulsating axial loading are carried out through finite element in the paper (Rizzetto et al., 2019). In study (Wang et al., 2022), the method of finite elements for investigating the failure mechanisms of cylindrical shells under internal explosion shock waves is used. In the paper (Yang, 2023) the buckling problem of cylindrical shells under combined non-uniform axial compression and external pressure is examined. A comprehensive overview of the behavior of cylindrical shell structures under different loading conditions, including external pressure, axial compression, and bending moment is provided in the research work (Ganendra et al., 2023).

However, the problem of studying the dynamic behavior of composite structures is far from being completely solved. Therefore, the development of analytical and numerical methods that allow to solve at least individual problems holds significant value. This underscores the relevance of developing techniques that enable conducting multiple numerical experiments to comprehensively study the dynamic behavior of composite structures.

2. Method

The dynamic deformation of a shell structure under the action of an external distributed load is considered. The structure under study is a fairing. It is represented as a hemisphere connected to a cylinder. The radius of the hemisphere is equal to R. The length of the cylinder and its radius are L and R, respectively. The edge of the cylinder is rigidly restrained ($u = w = \varphi = 0$).

The mathematical model of the processes of forced vibrations of the considered construction is reduced to the consideration of a hyperbolic system of nonlinear differential equations of the theory of shells and curvilinear rods of the Timoshenko type.

According to Timoshenko's theory of shells, geometric relations for nonlinear symmetric deformation of the body take the following form (Vorob'ev et al., 1989):

ISSN: 2456-3676

$$\varepsilon_{11} = \frac{\partial u_1}{\partial s} + k_1 u_3 + \frac{1}{2}\Theta_1^2,\ \varepsilon_{22} = \frac{u_1}{A_2}\frac{\partial A_2}{\partial s} + k_2 u_3,\ \varepsilon_{1Z} = \varphi + \Theta_1,\ \Theta_1 = \frac{\partial u_2}{\partial s} - k_1 u_1, \quad (1)$$

$$\chi_{11} = \frac{\partial \varphi}{\partial s}, \chi_{22} = \frac{\varphi}{A_2}\frac{\partial A_2}{\partial s}, \quad (2)$$

Where $k_i = \frac{1}{R_i}$, $s = \alpha_1 \cdot A_1$; A_1, A_2 are the coefficients of the first quadratic form of the surface that are responsible for the geometric parameters of the shell; u_1, u_3, φ are the components of the generalized displacement vector.

The forces and moments are given by the following formulas:

$$\begin{aligned} N_{11} &= B_{11}(\varepsilon_{11} + \nu_2 \varepsilon_{22}), \\ N_{22} &= B_{22}(\varepsilon_{22} + \nu_1 \varepsilon_{11}), \\ M_{11} &= D_{11}(\chi_{11} + \nu_2 \chi_{22}), \\ M_{22} &= D_{22}(\chi_{22} + \nu_1 \chi_{11}), \\ Q_{1Z} &= k^2 G_{1Z} h \varepsilon_{1Z}, \end{aligned} \quad (3)$$

where G_{1Z} is the shear modulus in the plane $z = const$, ν_1, ν_2 are Poisson's ratios in the directions α_1 and α_2, respectively, k^2 is the shear correction factor,

$$B_{11} = \frac{E_1 h}{1 - \nu_1 \nu_2},\ B_{22} = \frac{E_2 h}{1 - \nu_1 \nu_2},\ D_{11} = \frac{E_1 h^3}{12(1 - \nu_1 \nu_2)}, \qquad D_{22} = \frac{E_2 h^3}{12(1 - \nu_1 \nu_2)}, \quad (4)$$

where E_1, E_2 are Young's moduli in the directions α_1 and α_2, respectively, h is the thickness of the shell.

The equations of motion have the following form:

$$\begin{aligned} &\frac{1}{A_2}\left[\frac{\partial}{\partial s}(A_2 N_{11}) - \frac{\partial A_2}{\partial s} N_{22}\right] + k_1 Q_{1Z} + P_1 = \rho h \frac{\partial^2 u}{\partial t^2}, \\ &\frac{1}{A_2}\left[\frac{\partial}{\partial s}(A_2 M_{11}) - \frac{\partial A_2}{\partial s} M_{22}\right] - Q_{1Z} + P_2 = \frac{\rho h^3}{12}\frac{\partial^2 \varphi}{\partial t^2}, \\ &\frac{1}{A_2}\frac{\partial}{\partial s}(A_2 N_{11}) - k_1 N_{11} - k_2 N_{22} + P_3 = \rho h \frac{\partial^2 w}{\partial t^2}, \end{aligned} \quad (5)$$

where ρ is the shell density, h is its thickness, P_i $(i = \overline{1,3})$ are the components of the generalized load vector, $u_1 = u$, $u_3 = w$.

ISSN: 2456-3676

Equations (1)–(5) can be reduced to the following system of the second-order differential equations:

$$\frac{\partial^2 u_i}{\partial x^2} - \frac{1}{c_i^2}\frac{\partial^2 u_i}{\partial t^2} = \sum_{j=1}^{n}\left(\alpha_{ij}u_j + \beta_{ij}\frac{\partial u_j}{\partial x}\right) \equiv F_i\,,\ (i=1,2,3)\,, \qquad (6)$$

where c_i are the wave propagation speeds, α_{ij}, β_{ij} are the coefficients that include geometric and physical parameters of the components, F_i are the designation of the right-hand sides of the equations.

The system of second-order differential equations (6) can be solved by so-called grid-characteristic method (Magomedov & Kholodov, 1988; Danylchenko et al., 2013).

For numerical integration, at first it is necessary to find the equations of the characteristic directions (physical characteristics) and differential relations on them. A simple technique exists for this purpose, which involves defining the characteristic directions as those along which the values of the highest derivatives of the sought functions can be undefined, due to the potential for discontinuity.

By supplementing system (6) with expressions for the total differentials $\frac{\partial u_i}{\partial x}$ and $\frac{\partial u_i}{\partial t}$:

$$d\left(\frac{\partial u_i}{\partial x}\right) = \frac{\partial}{\partial x}\left(\frac{\partial u_i}{\partial x}\right)dx + \frac{\partial}{\partial t}\left(\frac{\partial u_i}{\partial x}\right)dt,\ i=\overline{1,3};$$
$$d\left(\frac{\partial u_i}{\partial t}\right) = \frac{\partial}{\partial x}\left(\frac{\partial u_i}{\partial t}\right)dx + \frac{\partial}{\partial t}\left(\frac{\partial u_i}{\partial t}\right)dt,\ i=\overline{1,3};$$

which hold true for any direction, a system of nine equations is obtained. Solving this system with respect to $\frac{\partial^2 u_i}{\partial x^2}$ yields:

$$\frac{\partial^2 u_i}{\partial x^2} = \frac{N}{M}\,,$$

ISSN: 2456-3676

where

$$M=\begin{vmatrix} 1 & 0 & -1/c_1^2 & 0 & 0 & 0 & 0 & 0 & 0 \\ dx & dt & 0 & 0 & 0 & 0 & 0 & 0 & 0 \\ 0 & dx & dt & 0 & 0 & 0 & 0 & 0 & 0 \\ 0 & 0 & 0 & 1 & 0 & -1/c_2^2 & 0 & 0 & 0 \\ 0 & 0 & 0 & dx & dt & 0 & 0 & 0 & 0 \\ 0 & 0 & 0 & 0 & dx & dt & 0 & 0 & 0 \\ 0 & 0 & 0 & 0 & 0 & 0 & 1 & 0 & -1/c_3^2 \\ 0 & 0 & 0 & 0 & 0 & 0 & dx & dt & 0 \\ 0 & 0 & 0 & 0 & 0 & 0 & 0 & dx & dt \end{vmatrix},$$

$$N=\begin{vmatrix} F_1 & 0 & -1/c_1^2 & 0 & 0 & 0 & 0 & 0 & 0 \\ d\left(\frac{\partial u_1}{\partial x}\right) & dt & 0 & 0 & 0 & 0 & 0 & 0 & 0 \\ d\left(\frac{\partial u_1}{\partial t}\right) & dx & dt & 0 & 0 & 0 & 0 & 0 & 0 \\ F_2 & 0 & 0 & 1 & 0 & -1/c_2^2 & 0 & 0 & 0 \\ d\left(\frac{\partial u_2}{\partial x}\right) & 0 & 0 & dx & dt & 0 & 0 & 0 & 0 \\ d\left(\frac{\partial u_2}{\partial t}\right) & 0 & 0 & 0 & dx & dt & 0 & 0 & 0 \\ F_3 & 0 & 0 & 0 & 0 & 0 & 1 & 0 & -1/c_3^2 \\ d\left(\frac{\partial u_3}{\partial x}\right) & 0 & 0 & 0 & 0 & 0 & dx & dt & 0 \\ d\left(\frac{\partial u_3}{\partial t}\right) & 0 & 0 & 0 & 0 & 0 & 0 & dx & dt \end{vmatrix}$$

This second derivative is undefined if both determinants N and M are equal to zero. If $M=0$ then expanding the determinant by Laplace's method yields:

ISSN: 2456-3676

$$\left\{c_1^2-\left(\frac{dx}{dt}\right)^2\right\}\left\{c_2^2-\left(\frac{dx}{dt}\right)^2\right\}\left\{c_3^2-\left(\frac{dx}{dt}\right)^2\right\}=0.$$

Setting each of the expressions in the braces to zero results in two families of physical characteristics:

$$\frac{dx}{dt}=\pm c_i.$$

The obtained characteristics are called C_i^+ and C_i^- - characteristics. Usually, the quantities c_i are called the speeds.

Taking into account that $N=0$, it can be obtained:

$$\left\{c_1^2F_1(dt)^2-d\left(\frac{\partial u_1}{\partial x}\right)dx+d\left(\frac{\partial u_1}{\partial t}\right)dt\right\}\left\{c_2^2-\left(\frac{dx}{dt}\right)^2\right\}\left\{c_3^2-\left(\frac{dx}{dt}\right)^2\right\}=0. \qquad (7)$$

Assuming speed c_1 is not equal to any other speed c_i, Equation (7) yields that along the directions $\frac{dx}{dt}=\pm c_1$ the following relations hold

$$d\left(\frac{\partial u_1}{\partial t}\right)\mp c_1 d\left(\frac{\partial u_1}{\partial x}\right)\pm c_1F_1dx=0. \qquad (8)$$

Equations (8) are called the characteristic equations along $\frac{dx}{dt}=\pm c_1$. It can be proven by passing to the limit that Equations (8) hold even if the value of c_1 is equal to one or more c_i. Analogously, the characteristic equations for the other speeds have been obtained:

$$d\left(\frac{\partial u_i}{\partial t}\right)\mp c_i d\left(\frac{\partial u_i}{\partial x}\right)\pm c_iF_idx=0.$$

Since only continuous u_i are considered, then $du_i=\frac{\partial u_i}{\partial x}dx+\frac{\partial u_i}{\partial t}dt$ along any direction.

Equations (6) are the second-order differential equations with respect to x and t. Therefore, for each of the variables u_i two initial and two boundary conditions must be specified. The correct initial conditions are the specification of all functions $\frac{\partial u_i}{\partial x}$ and $\frac{\partial u_i}{\partial t}$ along the initial line $t=0$. Note that specifying $\frac{\partial u_i}{\partial x}$ along the initial line $t=0$ is equivalent to specifying u_i on $t=0$.

Along each of the boundary lines $x=X_1$ and $x=X_2$ one boundary condition must be specified for each u_i. The correct boundary condition would be to set all u_i on $x=X_1$ and $x=X_2$.

If the characteristic equations of a system of hyperbolic differential equations are known, then they can be integrated numerically. Only the case $c_1=c_2$ will be considered. At first, to perform numerical computations, a grid of characteristic lines is constructed. Then, the characteristic equations and compatibility equations are written in the finite-difference form with respect to the values of the dependent variables at the nodal points of the grid. The obtained grid contains a lot of irregular nodal points for practical numerical calculations. For simplicity, only C_1^+ and C_1^- characteristics are used as the prime grid (Figure 1), where $c_1=\max(c_i)$, and the values of the dependent variables are calculated only at the nodal points of this grid.

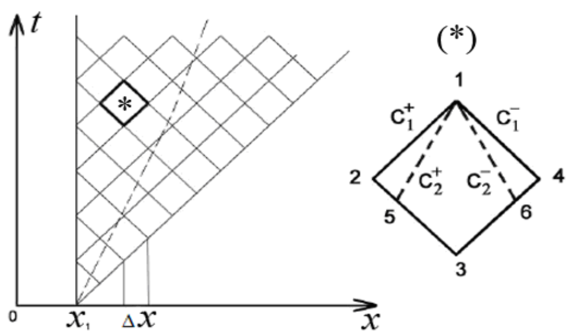

Figure 1. Grid of characteristic directions

The values of the variables u_i, $\frac{\partial u_i}{\partial x}$ and $\frac{\partial u_i}{\partial t}$ at the characteristic interior point 1 can be calculated based on the finite-difference form of four characteristic equations and two equations of compatibility, if their corresponding values at the neighboring points 2, 3 and 4 are known from previous calculations.

For the nodal points on the left boundary line $x=X_1$, the characteristics C_i^+ are absent. If u_i are specified on $x=X_1$, the remaining equations are sufficient for determining the unknowns $\frac{\partial u_i}{\partial x}$, $\frac{\partial u_i}{\partial t}$.

The sequence of calculations for determining the motion of elements in the composite structure is presented below.

1. The necessary data defining the geometric and physical characteristics of the investigated structure are prepared.
2. Assuming the initial state of the structure to be unperturbed, all unknown parameters are set to zero.
3. Values of parameters at the boundary points are computed. The data on the boundary are defined using boundary conditions, and the values of unknowns are determined from relationships on characteristics that do not extend beyond the integration domain.
4. The parameters of internal points for each region are calculated. If the required parameters are implicit functions, their values are found by the simple iteration method.
5. The values of the parameters at the points of the contact line points are computed. Formally, the contact point can be considered as composed of two distinct points, one belonging to region 1 and the other to region 2. The unknown parameters at this "formal" point are determined using interface conditions.

The obtained values of the wave field parameters are used as the initial values for computing the values of the sought variables at the nodes of the grid domain for the next time step, starting from point 3.
If the values of the displacement components at the nodes of the grid region are known, the stresses can be calculated using the relations between stresses and displacements.

For the considered problem in Equations (1)–(4) it is accepted $A_1 = 1$, $A_2 = R$, $k_1 = 0$, $k_2 = 1/R$ for the cylindrical part and $A_1 = R$, $A_2 = \sin\alpha_1$, $k_1 = k_2 = 1/R$ for the spherical part. Nonlinear terms were not taken into account in Equations (1).

3. Numerical results and its discussion

Calculations were performed for the structure with the following geometric, physical and mechanical parameters: $\frac{h}{R} = 0.02$, $L = R = 0.5$ m, $E = 7\cdot 10^{10}$ Pa, $\nu = 0.3$. The load was taken in the form:

$$P_3(t) = \begin{cases} P_0 + \dfrac{P_1 - P_0}{t_1}\cdot t, & t \le t_1, \\ P_0, & t > t_1, \end{cases}$$

where $P_0 = 0.216\cdot 10^5$ Pa, $P_1 = 0.132\cdot 10^5$ Pa, $t_1 = \frac{R}{c_0}$, c_0 is the speed of sound in air.

Figure 2 shows distribution of deflections at time $t \approx 3t_1$. The numerical results (curve 2), obtained by the method presented in this article, are in agreement with those obtained in (Lugovoi et al., 2006) (curve 1) for the values of deflections u_3 ($w = u_3$) at time $t \approx 3t_1$, i.e. after the wave has been reflected. Comparing the results has shown that there is a difference in the values of the studied quantities at several points, particularly at their maximum values.

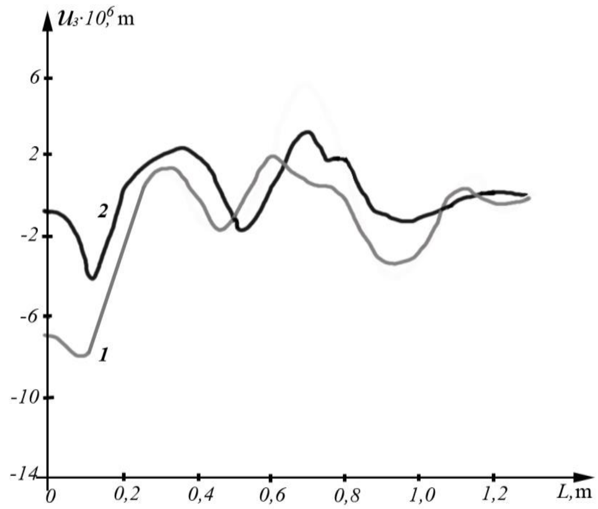

Figure 2. Distribution of deflections at time $t \approx 3t_1$

Calculations have shown that, as a result of diffraction of the load wave in the contact area between the components of the structure, the quantities under study experience a jump. By varying the geometric and mechanical parameters, it is possible to smooth out these jumps under the specific loading conditions. Using a transition curve in the interface area between the components of the structure, ensuring a smooth change of curvature, it is possible to achieve a decrease in stress concentration simultaneously with a decrease in the amount of material required to create these structures.

References

Danylchenko, D., Zasovenko, A., & Mastinovskiy, Y. (2013). Face Impact on Curved Axis Shell. *Herald of Aeroenginebuilding*, *1*, 46-49. http://journal.zntu.edu.ua/vd/files/VD12013/VD(1)_2013.pdf

Ganendra, B., Prabowo, A. R., Muttaqie, T., Adiputra, R., Ridwan, R., Fajri, A., Do, Q. Th., Carvalho, H., & Baek, S. J. (2023). Thin-walled Cylindrical Shells in Engineering Designs and Critical Infrastructures: A Systematic Review Based on the Loading Response. *Curved and Layered Structures*, *10*(1), 20220202. https://doi.org/10.1515/cls-2022-0202

Lugovoi, P. Z., & Meish, V. F. (1992). Numerical Simulation of the Dynamic Behavior of Reinforced Shells of Revolution under Nonstationary Loading. *Prikladnaya Mekhanika, 28*(1), 38-44.

Lugovoy, P. Z., Meish, V. F., & Shtancel', S. E. (2005). Forced Nonstationary Vibrations of a Sandwich Cylindrical Shell with Cross-Ribbed Core. *International Applied Mechanics, 41*(2), 161-167. https://doi.org/10.1007/s10778-005-0072-x

Lugovoi, P. Z., Meish, V. F., Rubakin, B. P., & Sekrieru, G. V. (2006). Dynamics of Reinforced Compound Shells under Nonstationary Loads. *International Applied Mechanics, 42*(4), 455-460. https://doi.org/10.1007/s10778-006-0102-3

Magomedov, K. M., & Kholodov, A. S. (1988). *Grid-Characteristic Numerical Methods*. Moscow, Nauka.

Meish, V. F. (2005). To the Numerical Solving the Problems of Dynamics of Stiffened Ellipsoidal Shells under Non-Stationary Loads. *International Applied Mechanics, 41*(4), 386-391. https://doi.org/10.1007/s10778-005-0100-x

Meish, V. F., & Kairov, A. S. (2005). Vibrations of Reinforced Cylindrical Shells with Initial Deflections under Nonstationary Loads. *International Applied Mechanics, 41*(1), 42-48. https://doi.org/10.1007/s10778-005-0056-x

Meish, V., Meish, Yu., & Belova, M. (2020). Nonstationary Dynamics of Elliptic Isotropic Conical Shells Under Distributed Loads. International Applied Mechanics, 56, 424-431. https://doi.org/10.1007/s10778-020-01026-6.

Myachenkov, V. I., & Grigoriev, I. V. (1981). *Calculation of composite shell structures on a computer. Handbook of Mechanical Engineering*. Moscow.

Naval, N. K., Patsyuk, V. M., & Rimsky, V. K. (1986). *Nonstationary waves in deformable media*. Chisinau, Shtiintsa.

Rizzetto, F., Jansen, E., Strozzi, M., & Pellicano, F. (2019). Nonlinear dynamic stability of cylindrical shells under pulsating axial loading via transient Finite Element Analysis. *Thin-Walled Structures*, *143*, 106213. https://doi.org/10.1016/j.tws.2019.106213

Shulga, N. A., & Bogdanov, S. Y. (2003). Forced Axisymmetric Nonlinear Vibrations of Reinforced Conical Shells. *International Applied Mechanics, 39*(12), 1447-1451. https://doi.org/10.1023/B:INAM.0000020829.56530.22

Vorob'ev, Yu. S., Kolodyazhnyi, A. V., Sevryukov, V. I., & Yanyutin, E. G. (1989). *High-Speed Deformation of Structural Members*. Kiev, Naukova Dumka.

Wang, D., Qin, X., Chen, W., & Wang, S. (2022). Simulation of the Deformation and Failure Characteristics of a Cylinder Shell under Internal Explosion. *Applied Sciences*, *12*, 1217. https://doi.org/10.3390/app12031217

Yang, L. (2023). Analytical Investigation on the Buckling of Cylindrical Shells under Combined Non-uniform Axial Compression and External Pressure. *Proceedings of the Institution of Mechanical Engineers, Part C: Journal of Mechanical Engineering Science, 237*(24), 6009-6019. https://doi.org/10.1177/09544062231168727